Experimental Validation of Foot to Foot Range Measurements in Pedestrian Tracking

Michel Laverne, Michael George, Dale Lord, Alonzo Kelly, Tamal Mukherjee, Carnegie Mellon University

BIOGRAPHY

Michel Laverne is a Robotics Engineer at Carnegie Mellon University's National Robotics Engineering Center in Pittsburgh, PA. He received his Master's degree in Computer Sciences and Modeling from the Institut Supérieur d'Informatique, de Modélisation et de leurs Applications in Clermont-Ferrand, France in 2006. Before joining CMU, he worked on the modeling and simulation of large complex information systems at the National Institute of Standards and Technology in Gaithersburg, MD. He also contributed to the hardware and software development for the detectors of the LHCb experiment at CERN in Geneva, Switzerland. His research interests include embedded systems, sensors and software for robotic applications.

Michael George is a Robotics Engineer at Carnegie Mellon University's National Robotics Engineering Center in Pittsburgh, PA. He received a Master's degree in Robotics from the Australian Center for Field Robotics at the University of Sydney in 2007. He works on inertial navigation and sensor fusion for pedestrian navigation and ground robots.

Dale Lord is a Robotics Engineer at Carnegie Mellon University's National Robotics Engineering Center in Pittsburgh, PA. He received his Bachelors, Masters, and PhD at the University of Missouri - Rolla. He is currently the Planning Lead of the Autonomous Haulage System Program at the NREC. His interests include planning, perception and position estimation for mobile robotic systems.

Alonzo Kelly is an Associate Professor at the Robotics Institute of Carnegie Mellon University. He received his B. A. Sc. in Aerospace engineering from University of Toronto in 1984, his B. Sc. in computer science from York University in 1990, and his Masters and Ph.D. degrees in robotics from Carnegie Mellon University in 1994 and 1996 respectively. His research interests include perception, planning, control, simulation, and operator interfaces for indoor and outdoor mobile robots.

Tamal Mukherjee is a Professor at the Electrical and Computer Engineering Department of Carnegie Mellon University. He received the B.S., M.S., and Ph.D. degrees in Electrical and Computer Engineering from Carnegie Mellon University in 1987, 1990, and 1995 respectively. His research interests include design techniques and methodologies at the boundary of analog, RF, microelectromechanical systems and microfluidic systems. He is currently integrating MEMS inertial sensors with RF sensors for localization applications in GPS-denied environments. He is also exploiting CMOS-MEMS technologies for reconfigurable RF applications.

ABSTRACT

A pedestrian tracking system using inertial sensors mounted on both feet is presented. Significant accuracy improvements are demonstrated, compared to single shoe tracking, by using sonar foot-to-foot range measurements to constrain heading drift. A single complementary Kalman filter fuses data from both inertial measurement units and the sonar sensor. The system is composed of commercial and custom hardware. Experimental results collected over long durations and distances are presented.

INTRODUCTION

Pedestrian tracking is the problem of calculating the position and orientation of walking individuals with wearable devices. It can provide situational awareness for first responders, direct advertising at potential consumers, map resources or buildings, guide the visually impaired etc.

There are two approaches to pedestrian tracking in the current literature. Pedometry approaches count steps, and measure heading and step distance to resolve position [8]. The advantage of the pedometry approach is that sensors can be mounted anywhere on the body and that errors are typically only motion and not time dependent. One disadvantage is that a biomechanical model that is user dependent is typically needed to determine step length. Inertial navigation approaches implement a full six degree-of-freedom inertial solution at the foot and use each footfall to reset accumulated error [3][4][5]. The inertial approach requires sensors to be at the foot and exhibits errors that are both time and motion dependent. However, the solution is not user dependent and in fact is

almost identical to aided inertial navigation solutions for vehicle tracking so it can leverage a body of pre-existing work. The system and results described here use an inertial system.

Zero velocity updates at each footfall reduce the time dependence of position error variance from cubic to linear, when assessed independently of orientation effects. Zero velocity updates, however, cannot resolve heading error and heading gyro bias error [2]. More specifically, zero velocity updates cannot resolve the components of gyro bias parallel to the specific force vector [4]. When the foot is on the ground, during footfall, this specific force vector is approximately the gravity normal force. Hence the uncorrected gyro and orientation components are those that affect pedestrian heading. It has been shown that two independent inertial solutions, one on each foot, with a range constraint between them can largely remove these remaining heading and gyro bias errors [1]. This result however has only been reported in simulation studies. We present here, to our knowledge, the first experimental implementation of this idea and confirm significant accuracy improvements.

Left and right feet are tracked with independent IMUs and inertial solutions. A single complementary Kalman filter tracks errors in both solutions. Periods of zero velocity are inferred from acceleration signals and corrections are applied separately on each foot. A sonar sensing system is mounted alongside each IMU to measure range between the feet. With this measurement, errors on both sides are corrected and the two solutions become coupled via the covariance correlations maintained in the filter. In our experiments, without this range measurement, heading error grows linearly in time because of gyro bias, drift and dynamic response and differs for each foot. The addition of the range measurement reduces the heading error drift rate by up to an order of magnitude. The remaining trend is still generally linear in time but it is the same for both feet.

The system operates in a local coordinate frame that can be geo-located with the addition of initial position and north relative heading.

A variety of inertial sensors have been tested in field trials, the results described here use a pair of tactical grade MEMS IMUs. The tracking filter provides three axis position, velocity and orientation and, optionally, online calibration data for each IMU.

The remainder of this paper is organized as follows: We review the inertial navigation approach to pedestrian tracking and present our algorithms, as they would be applied to an IMU on one shoe. We then extend these algorithms to two IMUs and add a range measurement between them. The experimental hardware is presented

and an analysis of experimental results, especially in comparison to previously reported systems is provided.

IMU CALIBRATION

The IMUs are calibrated before experiments. This procedure happens with the IMUs mounted on the boots but not with the boots on the feet. Gyro calibration is straightforward. While at rest, the gyroscopes are measuring only the rotation of the earth, ω_{earth} , which is a function of latitude, λ .

$$\begin{bmatrix} \omega_x \\ \omega_y \\ \omega_z \end{bmatrix} = R \begin{bmatrix} \omega_{earth} \cos(\lambda) \\ 0 \\ -\omega_{earth} \sin(\lambda) \end{bmatrix}$$

R is a rotation matrix that converts navigation (A local level north, east, down frame) to IMU coordinates. To remove noise and small oscillations, the gyro measurements are averaged for 3 minutes. This averaging period should be selected based on the minimum of the Allan deviation (i.e. the bias stability) to ensure that the average is optimal. For our sensor, the bias to noise ratio is approximately 0.02, so careful selection of the averaging period is important. Figure 1 shows the Allan deviation for the three-axis gyro, with a minimum at approximately 3 minutes.

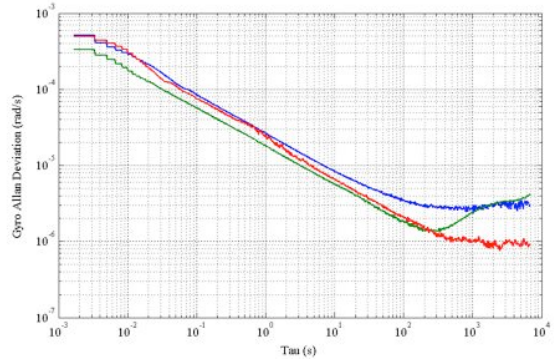


Figure 1. Allan deviation of the three-axis gyro. Averaging time in seconds, deviation in rad/s. Blue is the x IMU axis, green is y, red is z.

The difference between the average gyro readings and the expected earth rate signal is the calibrated bias.

$$\Delta \omega = \overline{\omega} - R \begin{bmatrix} \omega_{earth} \cos(\lambda) \\ 0 \\ -\omega_{earth} \sin(\lambda) \end{bmatrix}$$

This technique requires R, the navigation to IMU frame rotation, and latitude λ , to be known. The alignment section below shows how the calculation of R is accomplished using the accelerometer signals. Compared

to MEMS gyro accuracies, the earth rate variation with latitude is small, so an approximate value is sufficient.

Accelerometer calibration is more complicated. We use a method similar to [8]. The three axes of the accelerometer are sequentially exposed to positive and negative gravity normals while the IMU is stationary. See Figure 2.

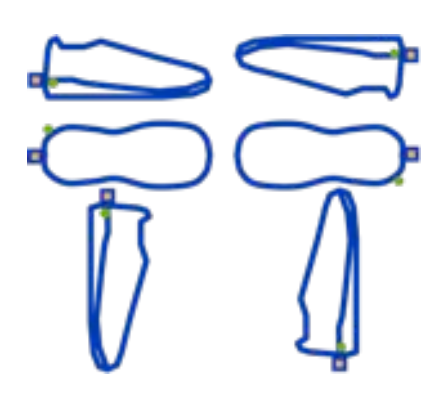


Figure 2. Six orientations required for the accelerometer calibration for a heel mounted IMU. Each face of the IMU bounding cube is pointed 'up'

The accelerometer readings are averaged for 3-5 seconds to give a total of six three-axis averages. An error term is calculated as the difference between the magnitude of the measured gravity signal, f, and the known magnitude of gravity at the current latitude, $g(\lambda)$

$$e = \left\| \overline{f} \right\| - g(\lambda)$$

The error term uses the vector norm and gravity magnitude and is one-dimensional. This is necessary since, roll and pitch angle errors are not separable from accelerometer biases in a static calibration [9]. A nonlinear optimization using the Levenberg-Marquardt algorithm is then used to minimize the error term while estimating the accelerometer biases, Δf .

The accelerometer calibration is performed before the gyro calibration because the accelerometer values are needed in the calculation of the R matrix.

The magnitude of gravity, including centripetal effects, at a given latitude is calculated from the WGS84 gravity model

$$g(\lambda) = g_{equator} \frac{1 + a_0 \sin^2(\lambda)}{\sqrt{1 - a_1 \sin^2(\lambda)}}$$

Where $g_{equator}$, the equatorial gravity, and a_0 and a_1 are constants [9].

ALIGNMENT

Each IMU measures three-axis specific force and threeaxis rotation rate. Given initial conditions, these signals can be integrated into position, velocity and orientation.

Initial position is either given to the system at startup by the user or set at (0,0,0), the latter implies a local reference frame. In both cases the navigation frame is a local level frame, suitable for navigation over several miles. For longer trajectories, the earth's curvature becomes important and would necessitate a reimplementation.

Initial velocity is assumed to be (0,0,0) in the navigation frame, meaning that the user must start with both feet stationary.

Initial orientation is determined in two steps. Roll and pitch angles (ϕ,θ) are calculated, while the user is wearing the boots and stationary, by computing the misalignment with the measured local gravity vector

$$\begin{bmatrix} f_x \\ f_y \\ f_z \end{bmatrix} = \begin{bmatrix} g(\lambda)\sin\theta \\ -g(\lambda)\cos\theta\sin\phi \\ -g(\lambda)\cos\theta\cos\phi \end{bmatrix}$$

Inverting

$$\begin{bmatrix} \phi \\ \theta \end{bmatrix} = \begin{bmatrix} \tan^{-1}(-\overline{f}_y, -\overline{f}_z) \\ \tan^{-1}(\overline{f}_x, \sqrt{\overline{f}_y^2 + \overline{f}_z^2}) \end{bmatrix}$$

Initial heading, ψ , is a user input since MEMS gyroscope technology is not yet capable of gyro-compassing. If initial heading is unknown it defaults to true north and degrades performance a small amount for failing to correct for the rotation of the navigation frame with Earth. This effect, at moderate latitudes, is generally less than 10 degrees/hour. That is significant in our case.

Roll, pitch and heading angles are then converted to the rotation matrix, R, relating the navigation frame and the IMU frame [9].

INS MECHANIZATION

The alignment stage described above gives initial conditions for the inertial solution recursions. For orientation

$$R_k^T = R_{k-1}^T \mathbf{A}$$

Where k is a time and data index determined by the IMUs in use or the algorithm design. In this case each k is 1/600s. A is an update matrix, composed of the small angle rotation between time indices, α , where

$$\mathbf{A} = \left(I + \frac{\sin\|\alpha\|}{\|\alpha\|} \left[\alpha \times \right] + \frac{1 - \cos\|\alpha\|}{\|\alpha\|^2} \left[\alpha \times \right]^2\right)$$

Superscript T represents matrix transpose, implying that the update increments the IMU to navigation rotation matrix rather than vice versa. The $[\alpha x]$ notation represents the cross product matrix. This is output by some IMUs directly or can be approximated to first order by

$$\alpha = \Lambda T \omega$$

Velocity is updated with

$$v_k = v_{k-1} + \Delta T \left(R^T f_{k-1} + g - 2\omega_{earth} \times v_{k-1} \right)$$

where g is gravity (The WGS84 model given above), ω_{earth} is earth rate and its cross product with velocity is the coriolis force. R is known from orientation recursion given above. The accelerometer output, f, is the specific force and ΔT is the time increment.

Position is integrated using a trapezoidal algorithm with the current and previous velocity

$$p_k = p_{k-1} + \frac{1}{2}\Delta T(v_k + v_{k-1})$$

Typical performance of free inertial navigation on a shoe depends on two principal factors. The first is the quality of the IMU, as disclosed by the manufacturer in a datasheet. The second is the IMUs response to the dynamics of the foot, which do not resemble any environment that commercially available IMUs are designed for. These second errors may be partially predicted by g-dependent gyro biases and various other terms that some manufacturers specify. In our experience the performance of a particular IMU on the foot is often not predictable without experimental data.

The IMUs used here are Honeywell HG1930 MEMs IMUs. Typical rated performance is 10 deg/hr gyro bias stability, which sets a performance flaw for free navigation with a calibrated gyro. Based on Allan deviation analysis, the particular models used here have bias stabilities closer to 3 deg/hr, See Figure 1. We observe this level of performance in the gyros when mounted on the torso, but typically observe 10-100x more drift error when mounted on the foot. Figure 3 compares

the heading solution for two calibrated IMUs mounted in different locations on the body. The black signal is a torso mounted device, with a trend line demonstrating very little drift (Bias stability of 3 deg/hr is not observable here) while the blue signal from a foot mounted device is accumulating heading error at approximately 135 deg/hr, well above datasheet predictions. A similar phenomenon has been reported previously [4]. As will be demonstrated in the experiments to come, heading error is the major source of position error in most tracking scenarios, so we expect that inertial devices designed for these environments or improved online calibrations will significantly improve future performance.

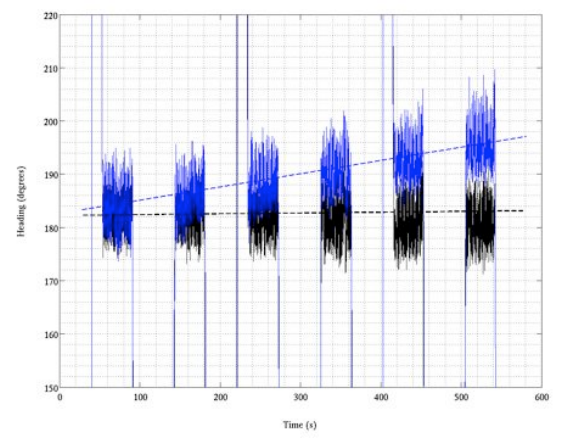


Figure 3. Heading drift rates of two calibrated IMUs. Black is torso mounted (0 deg/hr trend), blue is foot mounted (135 deg/hr trend).

To constrain drift error we use a complementary Kalman filter that maintains estimates of the error in the inertial states [13]. The filter requires a process model of the form

$$\dot{\mathbf{X}} = f(\mathbf{X}, \mathbf{W})$$

where X is a vector of relevant states and W are noise sources that reflect the uncalibrated errors remaining in the IMU. W is assumed zero mean and white, which can always be enforced by moving any structure into the state X, whether it be non-zero mean (bias) or non-white correlations (Gauss-Markov process). We typically work with two models, one that includes gyro and accelerometer bias in the state and one that does not. The extended state version can compensate for bias drift from the calibrated values but in practice it typically overfits residual motion in the zero velocity updates, so we prefer the simpler formulation and present the rest of the development with this form. The state consists of three orientation errors, forming a small angle deviation from the true orientation, three-axis position errors and threeaxis velocity errors.

$$X = \begin{bmatrix} \delta \Psi \\ \delta P \\ \delta V \end{bmatrix}$$

The noise sources represent three-axis gyro and accelerometer uncertainties that cover errors not initially calibrated

$$W = \left[\begin{array}{c} W_{\omega} \\ W_{f} \end{array} \right]$$

This represents the simplest model for uncertainty input into an inertial filter but it also the most robust without a more precise understanding of the dynamic error response of the IMU on the foot. Linearizing at the current state gives

$$\delta \dot{\mathbf{X}}\Big|_{\mathbf{X}_{k}} = F\mathbf{X} + G\mathbf{W}$$

where F and G are Jacobian matrices taken with respect to state and noise. In this case, these are

$$F = \begin{bmatrix} 0_{3\times3} & 0_{3\times3} & 0_{3\times3} \\ 0_{3\times3} & 0_{3\times3} & I_{3\times3} \\ \left[\left(R^T f \right) \times \right] & 0_{3\times3} & -2 \left[\omega_{earth} \times \right] \end{bmatrix}$$

and

$$G = \begin{bmatrix} -R^T & 0_{3\times 3} \\ 0_{3\times 3} & 0_{3\times 3} \\ 0_{3\times 3} & R^T \end{bmatrix}$$

The specification of X, F, G and the power spectrum of W is sufficient to predict system uncertainty using the standard Kalman filter relations, given initial uncertainties in each state. Initial roll and pitch uncertainties are derived from estimates of the residual accelerometer biases passed through the alignment equations. Heading, position and velocity uncertainties, like their mean values are user inputs.

Footfall, the period when a foot is flat on the ground while walking, is inferred from the following signal

$$zv = (var_n(f) < m)$$
? true : false

This should be interpreted as measuring the variance of the accelerometer signal (over the preceding n seconds) compared component wise with a threshold m. If each component is less than a than m, an indicator is true, otherwise it is false. Here n = 0.1s and $m = 0.1m^2/s^4$.

When the indicator variable is true, a footfall is detected and an assumption that the IMU is now at zero velocity is enforced in the filter. This takes the form of a Kalman update directly measuring the velocity error as the current inertial solution velocity estimate.

Many other zero velocity detectors are mentioned in the literature [7]. What is not mentioned is that these detection techniques mostly measure constant acceleration, which is then assumed to mean zero velocity. This is approximately true for foot-mounted sensors, when walking, because the complex dynamics of the foot mean velocity is never constant for n seconds except during footfall. This assumption fails however in elevators, on moving walkways and when the user is in a When it fails, the system non-accelerating vehicle. performance will degrade rapidly and may be unrecoverable. Our system has these failure modes also.

The threshold, m, needs to be set far above the noise floor of the accelerometers (0.1 m²/s⁴ vs. 0.0009 m²/s⁴) for any detections to occur. This implies that real motion of the foot is occurring which in turn implies that the zero velocity assumption is an approximation at best. Figure 4 shows the accelerometer and gyro signals over the period of one step (Approximately 1.2s) starting and ending at heel impact with the ground. At full scale the period 0.2-0.3 seconds appears to support the notion of constant acceleration.

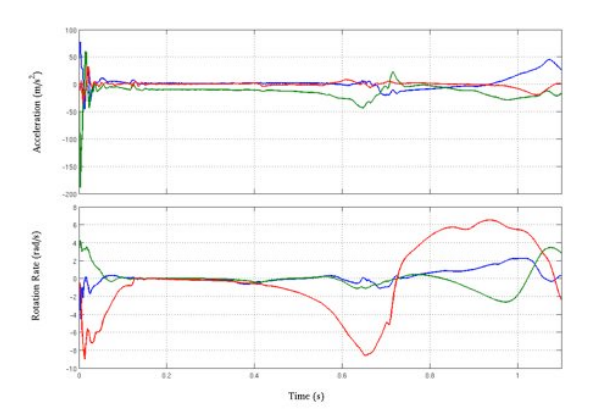


Figure 4. Accelerometer (upper) and gyro (lower) signals for the period of one step. The 0.2-0.3s window is typically assumed to be at zero velocity.

Figure 5 presents the x IMU axis accelerometer and gyro signals from the 0.2-0.3s window of Figure 4 at an enlarged scale. Overlaid on the signal is an indicator of the three-sigma noise values for reference (Red lines). It is obvious from this that real motion of the IMU is

occurring during footfall, with significant magnitude and structure in the signal. A truly zero signal would be 99% contained within the red lines.

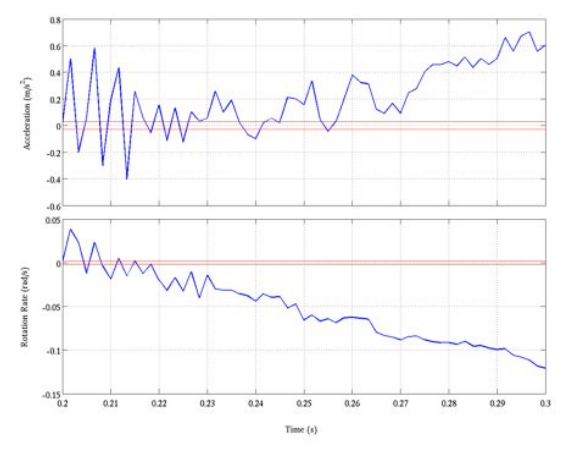


Figure 5. Accelerometer (upper) and gyro (lower) x axis signals during footfall (blue), enlarged view of the 02-0.3s window of Figure 4. Positive and negative 3 sigma noise bars (red) indicate real motion is present.

The Kalman filter assumes measurement errors are zero mean and uncorrelated in time so the accuracy of any zero velocity based system will be limited by this model fault. To improve upon the current technique we introduce the following model, which is intended to capture some of the motion of the IMU during footfall.

$$v_k^{imu} = \omega_k \times r_{toe \to imu}^{imu}$$

Where k is again a time and data increment and superscript IMU means the variable is measured in the IMU reference frame, not the navigation frame.

This model makes use of the accurate gyro signal, ω_k , plus a vector range from a point of pivot near the toes of the foot to the IMU center, $r_{toe_{\Rightarrow}imu}$. This is an assumption that IMU velocity when the foot is in contact with the ground can be described by pure rotation. The radius $r_{toe_{\Rightarrow}imu}$ will change as the footfall progresses from the heel to the toes. At present we detect heel impact, which presents an obvious spike in acceleration (See Figure 4, 0s mark) using a local maximum operator, then introduce a delay, calibrated to allow the transition from heel to forefoot to occur. The velocity model given above is then applied as the foot lifts off the ground, pivoting around the forefoot.

Not only does this model improve estimation of the velocity mean, it allows for more accurate introduction of uncertainty. Denoting covariance matrices by P we can write the uncertainty in the velocity as the transform of gyro and pivot radius uncertainties

$$P_{v} = [r_{toe \to imu} \times] P_{\omega} [r_{toe \to imu} \times]^{T} + [\omega \times] P_{r} [\omega \times]^{T}$$

The covariance of the gyro is known and the covariance of the radius is fixed to cover some portion of the forefoot depending on the accuracy of the impact detection and the delay function described above.

Because this measurement is formulated in the IMU reference frame, where ω and $r_{toe_{\Rightarrow}imu}$ are measured, the filter must relate velocity error to the states. This is accomplished by

$$\delta v = \begin{bmatrix} -R[v \times] & 0_{3 \times 3} & R \end{bmatrix} X$$

Extending the above algorithms to two shoes requires concatenating the state, noise input and Jacobians.

$$X' = \begin{bmatrix} X_{left}, X_{right} \end{bmatrix}^{T}$$

$$W' = \begin{bmatrix} W_{left}, W_{right} \end{bmatrix}^{T}$$

$$F' = \begin{bmatrix} F_{left}, F_{right} \end{bmatrix}^{T}$$

$$F' = \left[F_{left}, F_{right} \right]^{T}$$

$$G' = \left[G_{left}, G_{right} \right]^{T}$$

A sonar then measures the range between them, with the following model for range error

$$\delta r = \frac{1}{\|P_{left} - P_{right}\|} \begin{bmatrix} \left[\left(P_{right} - P_{left} \right) \times \right] I_{3x1} \\ \left(P_{left} - P_{right} \right) \\ 0_{3x1} \\ \left[\left(P_{left} - P_{right} \right) \times \right] I_{3x1} \\ \left(P_{right} - P_{left} \right) \\ 0_{3x1} \end{bmatrix} I_{3x1}$$

Where p is the position of the sonars, not the IMUs

$$p_{sonar} = p_{imu} + R^T r_{imu \to sonar}$$

HARDWARE

The system sensing is composed of two Honeywell HG1930 AA90 IMUs and a Devantech sonar range finder. These are connected to a Xilinx Virtex 4 FPGA with custom interface electronics. The FPGA implements the necessary communication protocols, receives, formats and timestamps incoming sensor data and then transmits it on a local network. A small form factor PC running Ubuntu Linux and our real-time positioning software performs the inertial navigation and filtering.



Figure 6. HG1930 IMU mounted on standard issue boot. Sonar transceivers (silver cylinders). Mil-spec connector runs cabling to backpack computing.

Figure 6 shows the IMU (brass cylinder) mounted on a boot. Two sonar transceivers (silver cylinders) at located nearby. An electrical and power interface board (green) connects to a mil-spec connector, which attaches to backpack computing and electronics. An exploded view of the entire system is shown in Figure 7.



Figure 7. Exploded view of entire system. The grey box contains electronics and computing and resides in the backpack. Cables connect IMUs and sonars at each foot. An iPad provides a user interface via WiFi. An alignment brace ensures the two IMUs have the same initial heading.

RESULTS

We present two experiments; the first is a continuous 4 hour repetitive path to demonstrate system reliability and accuracy. The second is a 2 hour freeform path with static intervals that simulates a typical office scenario where the user spends time at a desk and occasionally moves around an office building.

For indoor tracking, GPS cannot be used as a reference and for environments as large as our test locations there are no practical ground truth systems available. For the first test a known rectangle is followed for 4 hours, allowing the calculation of position error at each corner. The path length is approximately 20km consisting of 48 laps. Figure 8 shows the tracking solution (blue)

compared to the known path (red). Figure 9 shows root sum squared position errors at each corner.

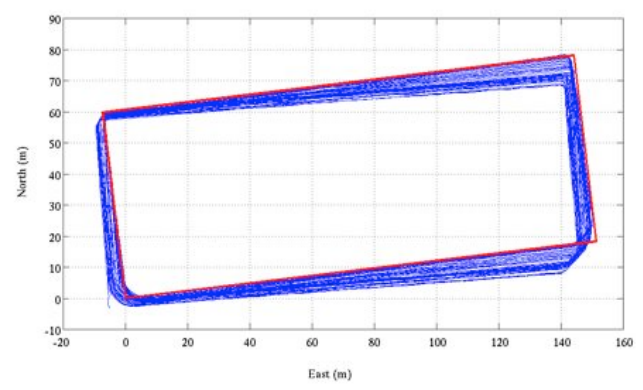


Figure 8. 2D rectangular path. Test duration is 4 hours and approx. 20km. Tracking solution (blue) is compared to known path (red).

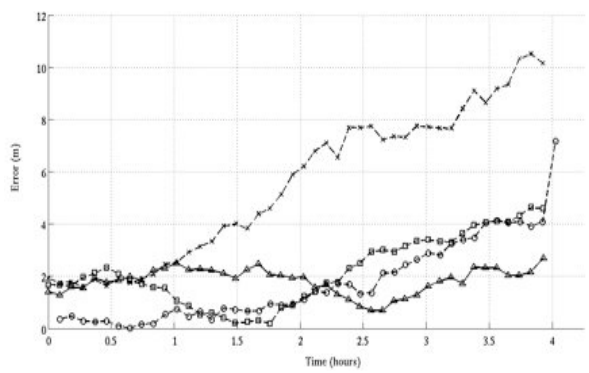


Figure 9. RSS Position error assessed at each corner of the path in Figure 8. Circles are corner 1, squares corner 2, crosses corner 3 and triangles corner 4. Corners are numbered counter-clockwise from the bottom left.

Position accuracy in this result is a function of heading error which is approximately 3.5 degrees after 4 hours, or less than 1 degree/hr heading drift. This improvement, compared to the gyro only performance shown in Figure 3, is a result of the sonar measurements ability to remove accumulated heading error. The maximum position error, 10.2m, occurs at corner 3 (top right). There is also a small scale factor error in the computed path that underestimates the true rectangle by approximately 1%. This result does not use the pivot velocity model described earlier and this underestimate is attributed to the zeroing of real motions during zero velocity updates. There are approximately 14,000 footfalls in a 4 hour experiment, so even 1mm of motion sums to a significant value.

Figure 10 shows the results of a simulated office scenario. In this case no ground truth is available but the result is overlaid on the office floor plan for comparison. Four

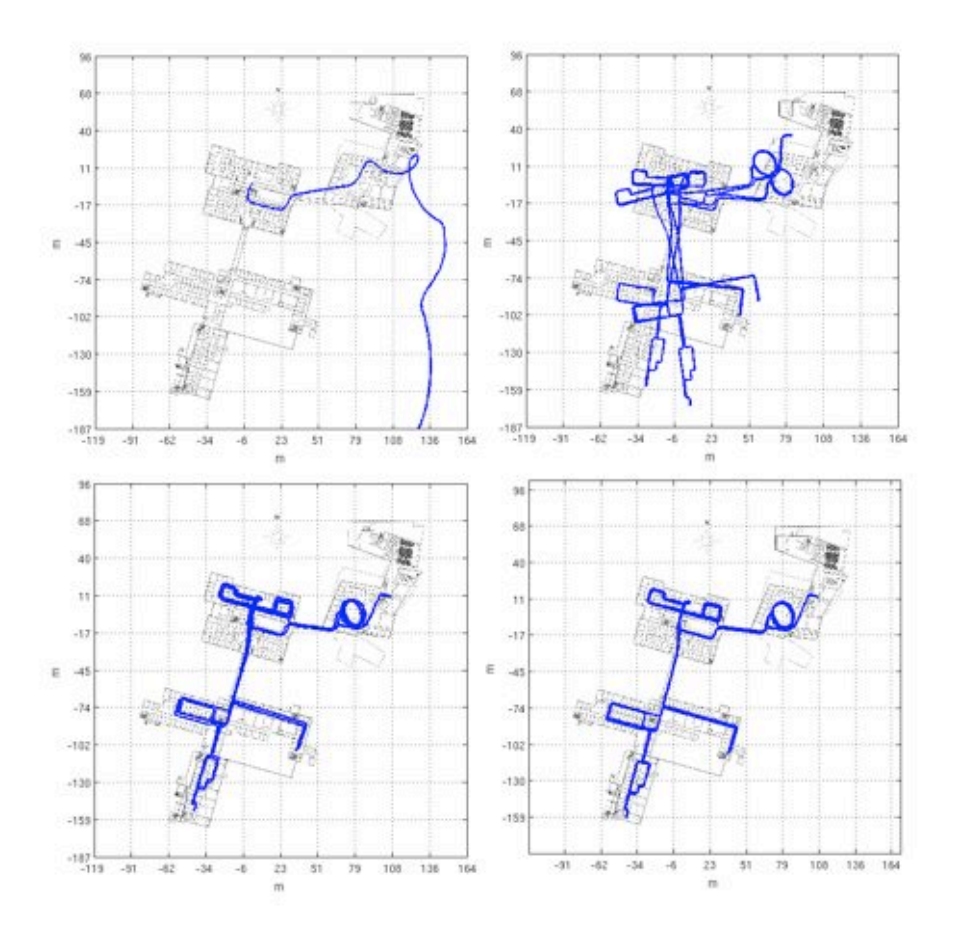


Figure 10. Simulated office scenario. The user spends 1.5 hours in the office in the top center of the images and 0.5 hours moving about the building. Top left shows free inertial. Top right is zero velocity updates without sonars, bottom left is zero velocity updates with sonars and bottom right is zero velocity updates, pivot velocity updates and sonars.

results are shown progressing from free inertial (top left). Standard zero velocity updates without sonar (tor right), standard zero velocity updates with sonar (bottom left) and standard zero velocity updates, pivot velocity updates and sonars (bottom right).

REFERENCES

- [1] T. J. Brand and R. E. Phillips, "Foot-to-foot range measurements as an aid to personal navigation," in Proceedings of the ION 59th Annual Meeting. Institute of Navigation, June 2003.
- [2] E. Foxlin, "Pedestrian tracking with shoe-mounted inertial sensors," IEEE Computer Graphics and Applications, vol. 25, no. 6, pp. 38–46, Nov.-Dec. 2005.
- [3] S. Wan and E. Foxlin, "Improved pedestrian navigation based on drift-reduced mems imu chip," in Proceedings of the ION 2010 International Technical Meeting, San Diego, USA, January 2010.
- [4] S. Hong, M. H. Lee, H.-H. Chun, S.-H. Kwon, and J. L. Speyer, "Observability of error states in gps/ins integration," IEEE Transactions on Vehicular

Technology, vol. 54, no. 2, pp. 731–743, March 2005.

- [5] B. Krach and P. Robertson, "Integration of foot-mounted inertial sensors into a bayesian location estimation framework," in Proceedings on the 5th Workshop on Positioning, Navigation and Communication. IEEE, 2008, pp. 55–61.
- [6] Z. Liu and C.-H. Won, "Knee and waist attached gyroscopes for personal navigation: Comparison of knee, waist and foot attached inertial sensors," in Position Location and Navigation Symposium (PLANS), 2010 IEEE/ION, May 2010, pp. 375 –381.
- [7] I. Skog, J.-O. Nilsson, and P. Handel, "Evaluation of zero-velocity detectors for foot-mounted inertial navigation systems," in Indoor Positioning and Indoor Navigation (IPIN), 2010 International Conference on, 2010, pp. 1–6.
- [8] I. Skog, P Händel, "Calibration of a MEMS inertial measurement unit" in IMEKO XVIII World Congress, 2006, Rio de Janeiro, Brazil.
- [9] J. Farrell, "Aided navigation: GPS with high rate sensors", 2008, McGraw Hill, NY.